Aging mechanisms analysis of Graphite/$LiNi_{0.80}Co_{0.15}Al_{0.05}O_2$ lithium-ion batteries among the whole life cycle at different temperatures

Wei Luo, *Xiaolong* Yang*, and *Sheng* Qiao

State Key Laboratory of Advanced Design and Manufacturing for Vehicle Body, Hunan University, Changsha, Hunan 410082, China

Abstract. Lithium-ion batteries (LIBs) are widely used in electric vehicles, while capacity fading happens due to unwanted side reactions during cycling. Therefore, it is of great significance to study the aging mechanisms of LIBs among the whole life cycle for the use and design of LIBs. In this study, the aging experiments of Graphite/$LiNi_{0.80}Co_{0.15}Al_{0.05}O_2$ (NCA) batteries were conducted at 25℃ and 45℃, the aging mechanisms were examined by differential voltage analysis method and electrochemical impedance spectroscopy analysis method, and verified by microscopic morphology observation. The results show that the loss of anode active material and lithium ions are the main degradation modes, and the lithium plating side reaction at the late aging stage is the inducement of capacity plunge both at 25℃ and 45℃. But the causes of lithium plating are different, at 25℃, the growth of solid electrolyte interphase (SEI) leads to lithium plating, while at 45℃, the accumulation of gas leads to lithium plating.

Keywords: Lithium-ion batteries, NCA/Graphite, Cycle aging, Degradation modes.

1 Introduction

LIBs have been extensively used in electric vehicles (EVs) due to their characteristics of high energy density, low self-discharge rate, and long cycle life [1]. However, during the cycling of LIBs, because of the change of internal structure and the occurrence of unwanted side reactions, such adverse phenomena as capacity attenuation, internal resistance rising, and power fading will occur [2]. The capacity attenuation will shorten the cruising range of EVs, the power fading will seriously affect the acceleration performance of EVs, and the rising of internal resistance will increase the heat generation of LIBs, which may lead to safety accidents without monitoring [3]. Therefore, it is very necessary to study the aging characteristics and mechanisms of LIBs.

* Corresponding author: 2689106523@qq.com

Compared with Graphite/$LiFePO_4$ (LFP) batteries, Graphite/NCA batteries have the advantages of higher energy density, better low-temperature performance, and are widely used in EVs [4, 5]. Many scholars have studied the cycle aging of Graphite/NCA batteries. Wong et al [6]. studied the aging performance of Graphite/NCA batteries at different discharge rates. Large discharge rates could accelerate the aging of LIBs, and pulse current discharge could make batteries age faster than constant current discharge. Waldmann et al. [7] studied the aging performance of Graphite/NCA batteries at different temperatures. From 0℃ to 60℃, the aging rate of LIBs gradually decreased with the increase of temperature. Wang et al. [8, 9] analyzed the aging mechanism of Panasonic 18650 Graphite/NCA batteries and proposed two schematic models. They believe that temperature would affect the decomposition products of the electrolyte in the battery, which are mainly solid at low temperature and gas at high temperature. This is the main reason why the decay rate of the battery at 60℃ is lower than 25℃. They also believe that the gradual thickening of SEI film would lead to the intensification of mechanical stress inside the electrode, which would increase the loss of electrode active material. However, these scholars only studied the aging influenced factors and the aging mechanism before the capacity plunge, most aging experiments were terminated when the capacity was delayed to about 80%, and the capacity plunge was rarely involved. But in the process of the practical application of LIBs, the echelon utilization of LIBs is also very important, so it's of great significance to study the aging mechanisms among the whole life cycle of LIBs [10, 11].

The characterization methods of aging mechanisms of LIBs could be divided into destructive characterization methods and non-destructive characterization methods. The destructive characterization methods are to disassemble the battery, observe the morphology, determine the element, and analyze the composition [12, 13]. Bhattacharya et al. [14] disassembled the recycled batteries and observed the growth pattern of SEI film on the anode surface using transmission electron microscopy. At 60℃, SEI film grows evenly and covers the anode surface rapidly. While at 25℃, SEI growth is inconsistent, it consumes a large amount of circulating lithium ions, making the capacity decay faster than 60℃; The non-destructive characterization methods are to analyze the degradation mode by using the external characteristic data of different nodes through the aging experiment [15, 16]. Differential voltage (DV) analysis and Electrochemical impedance spectroscopy (EIS) analysis are common non-destructive characterization methods. Zulke et al. [17] used the DV analysis method to study the degradation mode of Graphite/NCA batteries under a long rest time at different SOC and temperatures, they found that the main degradation mode of calendar aging was the loss of lithium ions caused by SEI film growth. Pastor-Fernandez et al. [18] studied the aging mechanisms of Graphite/NCA batteries at room temperature using the EIS analysis method, and the results showed that lithium ions loss and active material loss played a dominant role in batteries' aging, while conductivity loss had little influence.

This research used the Panasonic 18650 Graphite/NCA batteries, which were consistent with the experimental battery of Wang's research, [8, 9] to study the aging evolution of LIBs in the whole life cycle at different temperatures. Firstly, cyclic aging experiments were designed to record the battery capacity, internal resistance, impedance spectrum, and other external characteristics of each aging node. Then, the whole life cycle degradation mode of LIBs was analyzed qualitatively by the DV analysis method. Then, based on the EIS analysis method and the voltage relaxation behavior analysis method, the inducement of the capacity plunge was identified. Based on the analysis results and wang's presented models, the aging mechanism schematic models under different temperatures among whole life cycle were developed.

2 Experimental

The commercial cylindrical 18650 batteries made by Panasonic were tested for this research, the anode material of the battery is graphite, and the cathode material is $LiNi_{0.80}Co_{0.15}Al_{0.05}O_2$, other technical parameters are shown in Table 1. As shown in Figure 1, reference performance tests were carried out at 25℃ on the batteries firstly, including capacity calibration test, hybrid pulse power characteristic test, differential voltage test, voltage relaxation behavior test, and electrochemical impedance spectroscopy test. Taking battery capacity, internal resistance as consistency evaluation index, four batteries that have high consistency (deviation less than 1%) for the cyclic aging tests. Batteries (#1, #2) were cycled at 25℃, and batteries (#3, #4) were cycled at 45℃. The cycle conditions were set as follows: constant current charge to 4.2V at 1C and then constant voltage charge at 4.2V until current goes lower than 1/20C; rest 30 min; constant current discharge to 2.5V at 1C; rest 30 min. Reference performance tests were performed every 40 cycles for batteries (#1, #2), and every 60 cycles for batteries (#3, #4) until the capacity plunge was observed. The experimental equipment includes Shenzhen Neware battery testing system (CT-4008-5V50A-NTA), Xiamen East programmable constant temperature and humidity test chamber (ST-100LB), and Shanghai Chenhua Electrochemical Analyzer (CHI604E).

Table 1. Nominal specification of the test cell.

Item	Specification
Anode material/Cathode material	Graphite/$LiNi_{0.80}Co_{0.15}Al_{0.05}O_2$
Nominal capacity	3.25Ah
Nominal voltage	3.6V
Charge/Discharge cut-off voltage	4.2V/2.5V
Weight	48.5g
Gravimetric energy density	243Wh/kg

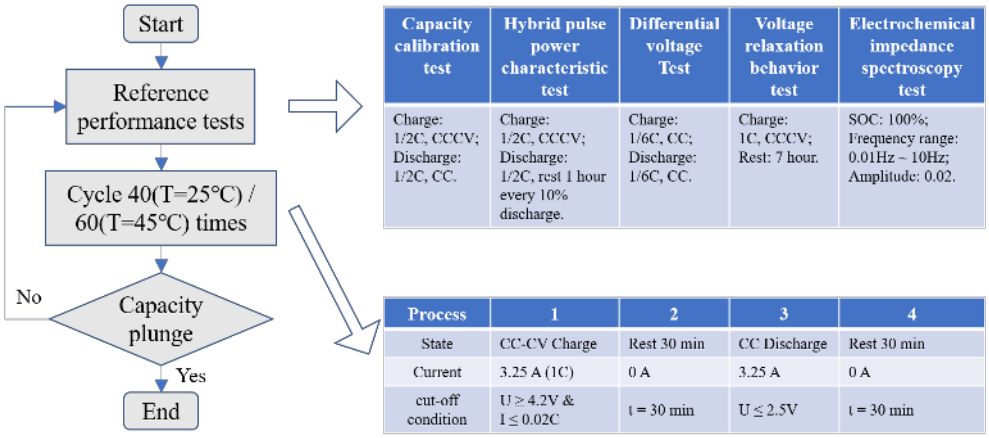

Fig. 1. The flow chart of the cyclic aging experiments.

3 Results and discussion

3.1 The analysis of capacity and resistance

The relative capacity attenuation curves and the internal resistance increase curves under 50%SOC are shown in Figure 2(a, b) respectively. For battery #1, capacity plunge occurs at

120 cycles, the first stage is 0-120 cycles, corresponding to the vehicle service life of the battery. The second stage is 120-160 cycles, at this time, capacity attenuation and internal resistance increase are more severe than the first stage, this stage corresponds to the battery echelon utilization stage. Capacity attenuation at 160 cycles is close to 50%, then the battery should be recycled constrainedly. For battery #2, the capacity attenuation is slower than that of battery #1, and the capacity plunge is delayed to 180 cycles.

3.2 The analysis of voltage relaxation behavior

According to related research, the lithium plating includes dead lithium and reversible lithium, reversible lithium will be embedded in the anode active particles or oxidized into the electrolyte during the rest period after charging, resulting in the appearance of voltage platform, and the trough on the dV/dt-t curve, which is known as voltage relaxation behavior, it is often used to determine whether lithium plating has occurred [19]. The voltage relaxation behavior analysis curves of batteries (#1, #3) are shown in Figure 2c and 2d respectively. The dV/dt-t curve shows a trough both at 120 cycles and 160 cycles, indicating that lithium plating occurs. The dV/dt-t curve of battery #3 showed a trough both at 180 cycles and 240 cycles, also indicating the existence of lithium plating. After the disassembly analysis of the fresh battery and the aged batteries (#1, #3), there are visible silver-white solids in the negative electrode (Figure 3), indicating that the lithium plating had occurred during cycling. Therefore, it can be preliminarily inferred that the capacity plunge of batteries at 25℃ and 45℃ may be caused by the lithium plating.

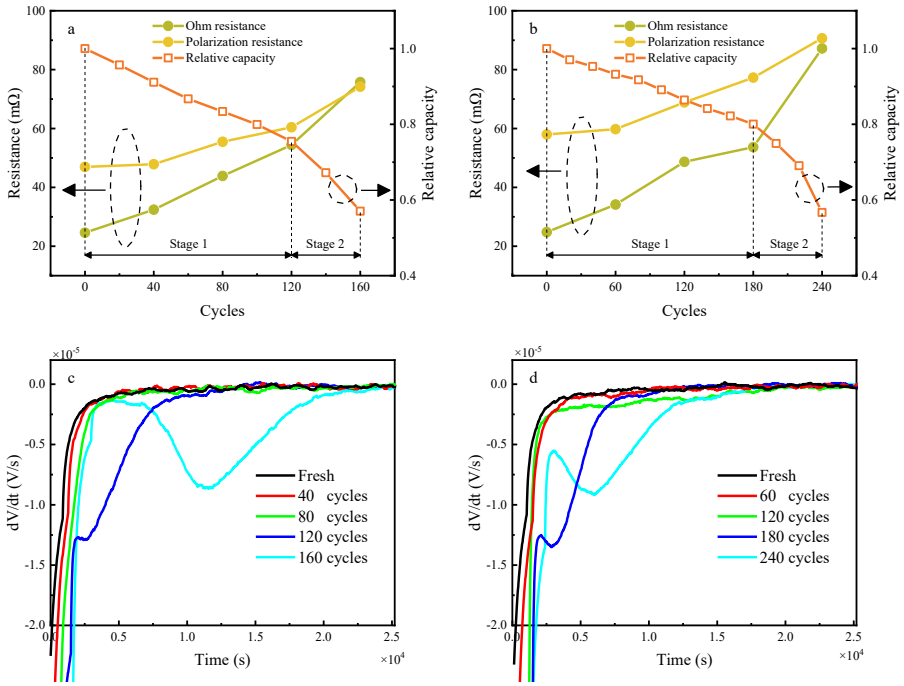

Fig. 2. The relative capacity attenuation curves and the internal resistance increase curves under 50%SOC of battery #1 (a), and battery #3 (b). The voltage relaxation behavior analysis curves at different cycles of battery #1 (c), and battery #3 (d).

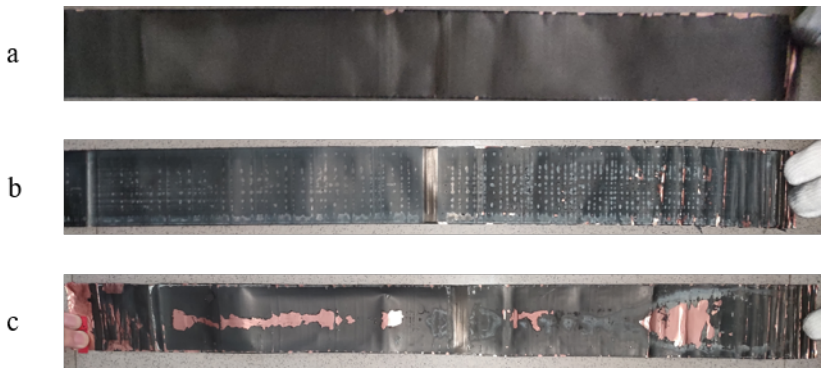

Fig. 3. The pictures of negative electrode surfaces: (a) Fresh battery; (b) Battery #1; (c) Battery #3.

3.3 The analysis of differential voltage

The DV analysis method is a common method for the non-destructive aging characterization of LIBs. The abscissa of the DV curve is capacity Q, and the ordinate is dV/dQ. Voltage and capacity are derived from 1/6C constant current charging data. Due to the phase transformation of the electrode in the process of Li+ intercalation/deintercalation, resulting in the formation of wave peaks on the DV curve. For lithium-ion batteries with Graphite/NCA system, according to relevant studies [17], its DV curve has three obvious peaks, as shown in Figure 4(a, b). Peaks P1 and P2 are determined by the negative electrode, while P3 is determined by the positive electrode. The loss of lithium ions and the loss of anode and cathode active materials can be determined by observing the offset of the peak. ΔQ1 (the change of Q1 which is the x-coordinate difference between 0%SOC and peak P2) reflects QL^{N}_{anode} (the anode capacity loss) caused by the loss of anode active materials during cycling. ΔQ3 (the change of Q3 which is the x-coordinate difference between peak P3 and 100% SOC) reflects QL^{N}_{cathod} (the cathode capacity loss) caused by the loss of cathode active material during the cycling, ΔQ2 (the change of Q2 which is the x-coordinate difference between P2 and 100%SOC) reflects QL^{N}_{ele} (the electrolyte capacity loss) caused by loss of lithium ions, and ΔQbatt (the change of Qcell) reflects QL^{N}_{batt} (the capacity loss of the battery) directly.

$$QL^{N}_{batt} = \Delta Qbatt = Q^{Fresh}_{batt} - Q^{N}_{batt} \quad (1)$$

$$QL^{N}_{anode} = \Delta Q1 = Q^{Fresh}_{1} - Q^{N}_{1} \quad (2)$$

$$QL^{N}_{ele} = \Delta Q2 = Q^{Fresh}_{2} - Q^{N}_{2} \quad (3)$$

$$QL^{N}_{cathode} = \Delta Q3 = Q^{Fresh}_{3} - Q^{N}_{3} \quad (4)$$

N represents the number of cycles.

As shown in Figure 4c, in the cycle aging process of battery #1, both QL^{N}_{ele}, QL^{N}_{anode}, and QL^{N}_{cathod} exist, of which the QL^{N}_{anode} is the main one, followed by QL^{N}_{ele}. In the first stage of aging (0-120 cycles), the QL^{N}_{batt} increases linearly, while the QL^{N}_{ele}, QL^{N}_{anode}, and QL^{N}_{cathod} also increase linearly. In the second stage of aging (120-160 cycles), the capacity plunges, and a significant increase in battery capacity loss is observed. The QL^{N}_{ele}, QL^{N}_{anode}, and QL^{N}_{cathod} also has dramatically increased, but still to QL^{N}_{anode} is given priority to, the second is QL^{N}_{ele}. As shown in Figure 4d, in the cycle aging process of battery #3, the loss of anode active material and the loss of lithium ions are the main. Compared with the

degradation mode at 25℃, the loss of anode active material decreases, and the loss of lithium ions increases at 45℃. Similarly, with the occurrence of the capacity plunge, the loss of each part will also increase under 45℃ cyclic aging.

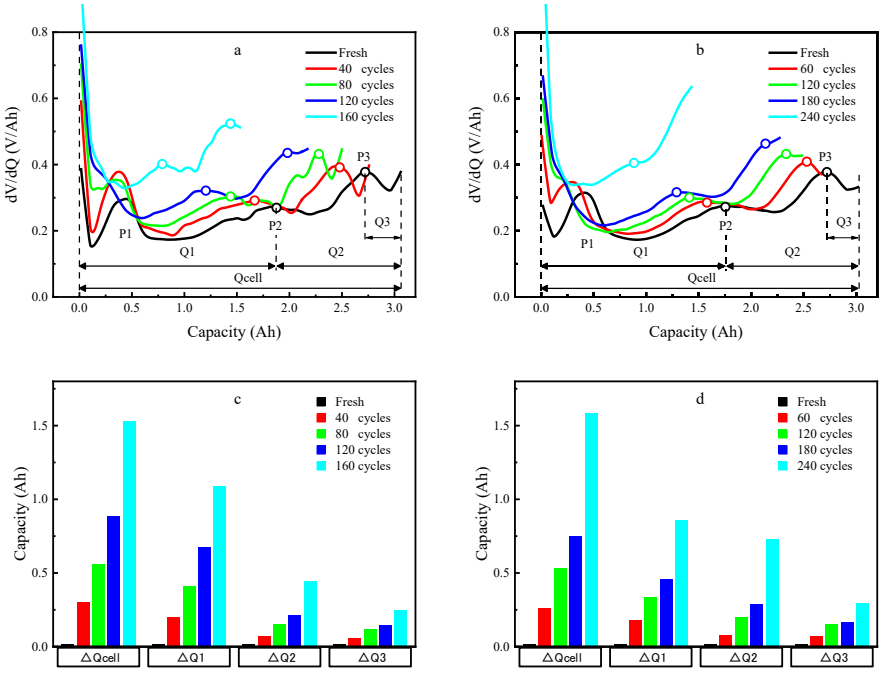

Fig. 4. The differential voltage curve at different cycles of battery #1 (a), and battery #3 (b). The capacity loss of each degradation mode at different cycles of battery #1 (c), and battery #3(d).

3.4 The analysis of electrochemical impedance spectroscopy

EIS is a powerful tool to study the mechanism of electrode interface reaction and capacity attenuation in LIBs. It can obtain the related electrochemical kinetic parameter and battery impedance by an equivalent circuit model. Figure 5a and 5b show the EIS curves of batteries (#1, #3) at 100%SOC under different cycles. It can be found that the EIS curve of LIBs consists of two semicircles and two lines. The semicircle in the high-frequency region is related to the SEI film impedance (R_{SEI}) of lithium battery, the semicircle in the low-frequency region is related to the charge transfer impedance (R_{ct}) of lithium battery, the oblique line in the high-frequency region is related to the ohm impedance (Rohm) of lithium battery, and the oblique line in the low-frequency region is related to the ion diffusion impedance (R_w) [18]. To better quantify the internal impedance of LIBs, the EIS curve was fitted with the 2RC equivalent circuit model. The change of R_{SEI} during cycling is shown in Figure 5c and 5d. It can be seen that in the cycle aging process at25℃, R_{SEI} impedance increases linearly in the first stage of aging. With the precipitation of lithium plating, a dense passivation film will be generated after lithium metal reacts with the electrolyte, which greatly increases R_{SEI}. In the process of the 45℃ cyclic aging process, R_{SEI} impedance decreases sharply at first and then flattens out.

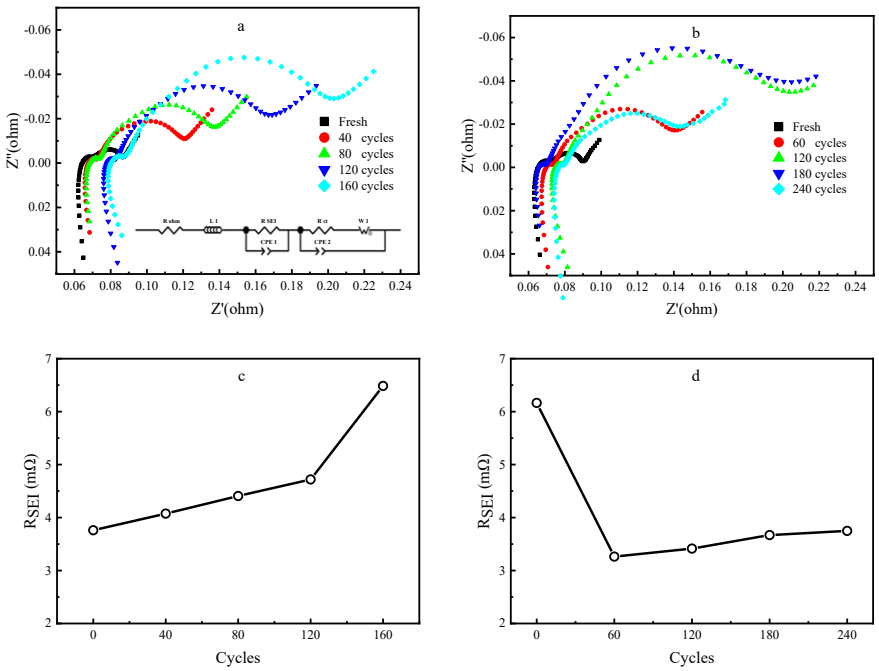

Fig. 5. The electrochemical impedance spectroscopy at different cycles of battery #1 (a), and battery #3 (b). The RSEI curve of battery #1 (c), and battery #3(d).

3.5 The discussion of aging mechanisms at different temperatures

According to relevant literature reports, the electrolyte decomposition of this type of battery has different products when circulating at different temperatures [8, 9]. At normal temperature, the electrolyte tends to decompose into solid components to form SEI film, while at high temperature, the electrolyte tends to decompose into gas. According to this view and the existing analysis, the following speculations can be made:

The degradation mechanisms at 25℃ are shown in Figure 6a, in the first stage, the electrolyte decomposed into SEI film and anode active material cracked are the main side reaction that causes capacity attenuation. With the increase of the SEI film, the anode surface film membrane resistance increases gradually, and anode electrode overpotential goes lower than 0V, then the lithium plating occurs. The lithium metal will react with electrolytes, and a dense passive layer will generate. The contact stress between electrode and separator is increased and the loss of active material is aggravated (the loss of anode active material is increased obviously) due to the dense passive layer. Therefore, the lithium plating is the inducement of capacity plunge, and the increase of lithium ions loss caused by continuous lithium plating and the aggravation of anode active material loss caused by the formation of passivation layer are the internal reasons for rapid capacity decay in the second stage of aging.

The degradation mechanisms at 45℃ are shown in Figure 6b, in the first stage, the electrolyte decomposed into gas and anode active material cracked are the main side reaction that caused capacity attenuation. The accumulation of gas at the gap of anode active material hindered the diffusion of lithium ions in the liquid phase, and lithium plating occurs. Then the passivation layer will also form. At the same time, the contact stress between the electrode and separator is increased, and the loss of active materials is

aggravated, which further leads to the phenomenon of capacity plunge, and also leads to the rapid decay of capacity in the second stage of aging.

The capacity plunge phenomenon at 25℃ and 45℃ is caused by lithium plating, and the capacity attenuation aggravated in the second stage of aging is caused by the loss of lithium ions caused by continuous lithium plating and the loss of active materials caused by the formation of the passive layer. The difference is that the inducement of lithium plating at 25℃ is the growth of SEI film, while the inducement of lithium plating at 45℃ is the accumulation of gas.

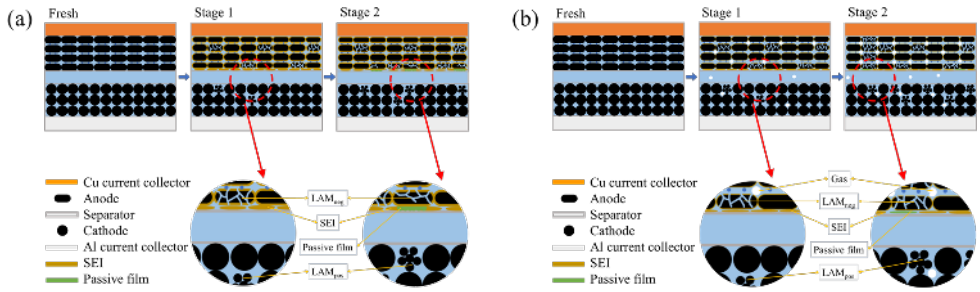

Fig. 6. The cycling degradation mechanism of battery at 25℃ (a), and 45℃ (b).

4 Conclusion

In order to study the aging mechanisms of graphite/NCA lithium-ion batteries among the whole life cycle at different temperatures, cycle aging tests were carried out at 25℃ and 45℃ respectively. Differential voltage analysis, electrochemical impedance spectrum analysis and morphology observation analysis were used to characterize the corresponding aging mechanisms. The results show that there are two stages of aging of graphite/NCA lithium-ion batteries at either 25℃ or 45 ℃. The first stage of aging is slow, and the main degradation mode is the loss of anode active material and lithium ions. As the cycle continues, lithium plating occurs on the anode surface, consuming a large amount of recyclable lithium ions. The subsequent formation of the passivation layer will increase the internal stress of the electrode, leading to the loss of active material. These side reactions together lead to the capacity plunge, and thus enter the second stage of aging with severe capacity attenuation. At 25℃, the thickening of SEI film leads to lithium plating, while at 45℃, the gas accumulation caused by side reaction leads to lithium plating. This study provides a new idea for the design of long-life battery, which can reserve the gap between various components in the battery. When the passivation film is formed, the small stress in the battery is not enough to increase the loss of active material, so as to prolong the service life of the battery. At the same time, the evolution process of aging mechanism in the whole life cycle is studied, which provides a theoretical basis for the establishment of mechanism aging model.

This work was supported by the National Natural Science Foundation of China [grant numbers 51775179].

References

1. Yoshino A. The birth of the lithium‐ion battery[J]. Angewandte Chemie International Edition, 2012, 51(24): 5798-5800.
2. Arora P, White R E, Doyle M. Capacity fade mechanisms and side reactions in lithium‐ion batteries[J]. Journal of the Electrochemical Society, 1998, 145(10): 3647.
3. Han X, Lu L, Zheng Y, et al. A review on the key issues of the lithium ion battery degradation among the whole life cycle[J]. ETransportation, 2019, 1: 100005.
4. Chen Y, Song S, Zhang X, et al. The challenges, solutions and development of high energy Ni-rich NCM/NCA LiB cathode materials[C]//Journal of Physics: Conference Series. IOP Publishing, 2019, 1347(1): 012012.
5. Blomgren G E. The development and future of lithium ion batteries[J]. Journal of The Electrochemical Society, 2016, 164(1): A5019.
6. Wong D, Shrestha B, Wetz D A, et al. Impact of high rate discharge on the aging of lithium nickel cobalt aluminum oxide batteries[J]. Journal of Power Sources, 2015, 280: 363-372.
7. Waldmann T, Kasper M, Wohlfahrt-Mehrens M. Optimization of charging strategy by prevention of lithium deposition on anodes in high-energy lithium-ion batteries–electrochemical experiments[J]. Electrochimica Acta, 2015, 178: 525-532.
8. Wang H, Frisco S, Gottlieb E, et al. Capacity degradation in commercial Li-ion cells: The effects of charge protocol and temperature[J]. Journal of Power Sources, 2019, 426: 67-73.
9. Wang H, Whitacre J F. Inhomogeneous aging of cathode materials in commercial 18650 lithium ion battery cells[J]. Journal of Energy Storage, 2021, 35: 102244.
10. Zhang Y, Li Y, Tao Y, et al. Performance assessment of retired EV battery modules for echelon use[J]. Energy, 2020, 193: 116555.
11. Xu X, Mi J, Fan M, et al. Study on the performance evaluation and echelon utilization of retired LiFePO4 power battery for smart grid[J]. Journal of Cleaner Production, 2019, 213: 1080-1086.
12. Zhang G, Wei X, Han G, et al. Lithium plating on the anode for lithium-ion batteries during long-term low temperature cycling[J]. Journal of Power Sources, 2021, 484: 229312.
13. Lang M, Darma M S D, Kleiner K, et al. Post mortem analysis of fatigue mechanisms in $LiNi_{0.8}Co_{0.15}Al_{0.05}O_2$–$LiNi_{0.5}Co_{0.2}Mn_{0.3}O_2$–$LiMn_2O_4$/graphite lithium ion batteries[J]. Journal of Power Sources, 2016, 326: 397-409.
14. Bhattacharya S, Riahi A R, Alpas A T. Thermal cycling induced capacity enhancement of graphite anodes in lithium-ion cells[J]. Carbon, 2014, 67: 592-606.
15. Raj T, Wang A A, Monroe C W, et al. Investigation of Path‐Dependent Degradation in Lithium‐Ion Batteries[J]. Batteries & Supercaps, 2020, 3(12): 1377-1385.
16. Pastor-Fernández C, Yu T F, Widanage W D, et al. Critical review of non-invasive diagnosis techniques for quantification of degradation modes in lithium-ion batteries[J]. Renewable and Sustainable Energy Reviews, 2019, 109: 138-159.
17. Zülke A, Li Y, Keil P, et al. High‐Energy Nickel‐Cobalt‐Aluminium Oxide (NCA) Cells on Idle: Anode‐versus Cathode‐Driven Side Reactions[J]. Batteries & Supercaps, 2021, 4(6): 934-947.

18. Pastor-Fernández C, Widanage W D, Marco J, et al. Identification and quantification of ageing mechanisms in Lithium-ion batteries using the EIS technique[C]//2016 IEEE Transportation Electrification Conference and Expo (ITEC). IEEE, 2016: 1-6.
19. Koleti U R, Rajan A, Tan C, et al. A study on the influence of lithium plating on battery degradation[J]. Energies, 2020, 13(13): 3458.